Numerical Simulation on Spreading and Impact Behavior of a Single Droplet Using Smoothed Particle Hydrodynamics

Hee Sang Yoo, Tae Hwan Kim, Eung Soo Kim*
Department of Nuclear Engineering, Seoul National University, 1 Gwanak-ro, Gwanak-gu, Seoul, South Korea
*Corresponding author: kes7741@snu.a.kr

1. Introduction

Most of nuclear reactors use coolant in liquid phase and the liquid might break up into small droplets in many components in nuclear power plants. The impact of these droplets into the solid wall is considered as one of the main causes of the degradation in nuclear piping. In addition, a design basis accident (eg. LOCA) or a severe accident (eg. FCI) generates lots of droplets that might collide with many nuclear reactor components including pipes, steam generators, containment and etc. Therefore, the deep understanding of the droplet-surface collisions has been of considerable interest for the comprehensive understanding of the degradation of components and accident scenarios in terms of nuclear safety [1].

In this respect, the numerous experimental and numerical studies have been complementary conducted. The majority of experimental studies have focused on the effect of various factors on the single droplet-surface collision phenomena, including the physical properties of droplet, velocity, collision angle, wetting characteristics, surface rigidity and etc. In addition, some experiments have been performed on multi-droplet or in form of jet. In order to illustrate the detailed information on droplet during the initial impact process such as the pressure, shape variance, distribution of secondary droplets which is still difficult in experimental studies, the numerical studies have been performed. Various numerical methods are adopted, which includes both mesh-based and mesh-free methods. The representative models of each method are MPS (moving-particle semi-implicit) and VOF (volume of fluid) [1].

In this study, various droplet-surface collision situations are analyzed thorough the 3D Smoothed Particle Hydrodynamics (SPH) [2]. For the physical and flexible expression on the surface tension and the surface wettability, the Pairwise Force SPH (PFSPH) model is adopted [3] has been shown that the SPH model can quantitatively and qualitatively cover the various droplet-surface collision situations in the nuclear engineering fields.

2. Smoothed Particle Hydrodynamics

The SPH is the most well-known Lagrangian mesh-free CFD method. Due to its Lagrangian nature, it has advantageous in handling the non-linear interface between multi phases and large deformations without interface tracking algorithm. In this section, the basic concept of SPH and discretized governing equations are briefly explained.

2.1 SPH approximation

In the basic principle of the SPH formulation, .a function $f(r)$ at a point r is approximated as the integral representation over a domain of interest Ω around a point r with a smoothing kernel function $W(x - x', h)$ as a weighting function.

$$f(r) = \int_{\Omega} f(r')W(r - r', h)dr' \tag{1}$$

The variable h represents the radius of the domain of interest Ω, so called as smoothing length. In the discretized system, the function $f(r_i)$ at the position of ith particle is expressed by

$$f(r_i) = \sum_{j} f(r_j)W_{ij}(r_i - r_j, h_i)V_j \tag{2}$$

where the subscript j represents the adjacent particles of ith particle, V is the volume of particle. The basic principle of the SPH approximation is described in Fig 1(a).
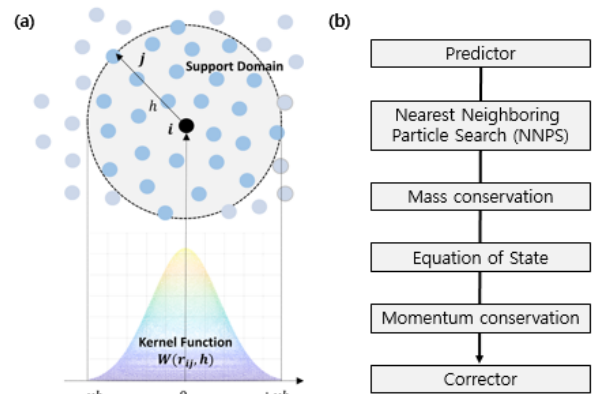

Fig. 1. SPH approximation and Overall algorithm

2.2 Governing equations

The governing equations for isothermal and incompressible flow include the mass equation and Navier-Stokes equation (momentum equation). Under the weakly compressible assumption, the pressure is explicitly calculated from the equation of state which is linearized along the compressibility of fluid. These equations are discretized by the SPH formulation in Table 1.

The mass equation (eqn (4)) is modified from its original form (eqn (3)) in order to accurately handle the

both single-phase and multi-phase with high density ratio. The each terms in N-S equation are the pressure force (eqn (5)), viscous force (eqn (6)) and the surface tension (eqn (7)), respectively.

In this study, the governing equations are integrated in time by 2nd predictor-corrector scheme. The overall algorithm is summarized in Fig 1(b).

Table I. SPH formulations for governing equations

Mass Equation
$$\rho_i = \sum_j \rho_j \frac{m_j}{\rho_j} W_{ij} \qquad (3)$$
$$\rho_i = \rho_{ref,i} \sum_j \frac{m_j}{(\rho_{ref})_j} W_{ij} \qquad (4)$$

Momentum Equation (Navier-Stokes Equation)
$$\left(\frac{\overrightarrow{du}}{dt}\right)_{fp,i} = -\sum_j m_j \left(\frac{p_i + p_j}{\rho_i \rho_j}\right) \nabla W_{ij} \qquad (5)$$
$$\left(\frac{\overrightarrow{du}}{dt}\right)_{fv,i} = \sum_j \frac{4m_j}{(\rho_i + \rho_j)} \frac{\mu_i \mu_j}{\mu_i + \mu_j} \frac{\overrightarrow{r_{ij}} \cdot \nabla_i W_{ij}}{\left(|\overrightarrow{r_{ij}}|^2 + \eta^2\right)} (\overrightarrow{u_i} - \overrightarrow{u_j}) \qquad (6)$$
$$\left(\frac{\overrightarrow{du}}{dt}\right)_{fs,i} = s_{ij} \cos\left(\frac{1.5\pi}{kh}|r_{ji}|\right) \frac{r_{ji}}{|r_{ji}|} \qquad (7)$$

Equation of State
$$p_i = \frac{c_{0i}^2 \rho_{0i}}{\gamma}\left[\left(\frac{\rho_i}{\rho_{0i}}\right)^\gamma - 1\right] \qquad (8)$$

3. Pairwise Force Smoothed Particle Hydrodynamics

The surface tension is one of the most important forces in multi-phase flows, particularly at the small scale. The Inter-Particle Force (IPF) model is proposed based on the microscopic origin of surface tension by assigning the force term between the particles [3] This force term acts as a repulsive force when two particles are close and act as an attractive force when two particles are far enough. Several force terms have been proposed, among which the cosine model is adopted. (eqn (7))

3.1 Surface tension

The surface tension is originated from the irregular distribution of molecules at the interface and the force imbalance induce the pressure jump across the interface. Therefore, some amount of energy has to be added to increase the interface area by a unit length, and this is the mechanical definition of surface tension. The mathematical expression of the definition of surface tension is known as Hardy formula (eqn (9))[3].

$$\sigma_{\alpha\beta} = \int_{-\infty}^{+\infty} [T_\tau(r) - T_n(r)]\, dr \qquad (9)$$

The $\sigma_{\alpha\beta}$ denotes the surface tension between phases α and β, T_τ and T_n are the tangential and normal stresses,

respectively, and the r direction represents the normal direction to the interface.

3.2 Wettability

In the equation 7, the s_{ij} is a parameter which controls the surface energy at the interface. The mathematical relation between this parameter and macroscopic wetting parameters (surface tension and contact angle) are derived using the mechanical definition of surface tension and summarized in Table II [3]

Table II. The relationship between microscopic parameter and macroscopic parameters [3]

Surface tension
$$\sigma_{\alpha\beta} = \lambda\left(n_\alpha^2 s_{\alpha\alpha} + n_\beta^2 s_{\beta\beta} - 2n_\alpha n_\beta s_{\alpha\beta}\right) \qquad (10)$$

Contact angle
$$\cos\theta_0 = \frac{\overline{s_{\beta\beta}} - \overline{s_{\alpha\alpha}} - 2\overline{s_{\beta s}} + 2\overline{s_{\alpha s}}}{\overline{s_{\alpha\alpha}} + \overline{s_{\beta\beta}} - 2\overline{s_{\alpha\beta}}} \qquad (11)$$

4. Results

4.1 Surface tension modeling

The multiphase SPH with surface tension model is verified with the pressure distribution of a single droplet. The figure 2(a) shows a water droplet surrounded by air phase at equilibrium. The pressure distributions perpendicular to the interface are shown in fig. 2(b) for droplets where the density ratios of water and air are 1 and 1000. A uniform pressure distribution is shown at bulk region and a pressure jump induced by microscopic origin is confirmed near the interface.
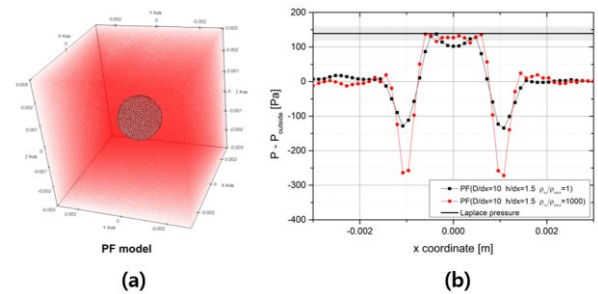

Fig. 2. A single droplet at equilibrium (a) The particle image (b) The pressure distribution

As described in section 3.2, the wettability of the surface can be controlled by adjusting s_{ij} in eqn (7). Figure 3 shows five different droplets on a surface. The contact angle of the droplets are 30°, 60°, 90°, 120°, and 150°, respectively. In the case of contact angles of 60°, 90°, 120°, and 150°, the theoretical contact angle and the measured contact angle showed good agreement with an error within 10%. The error of 25% is shown in the case

of 30°. The error may have occurred because the angle is too small to measure accurately.

Fig. 3. Droplets with different static contact angle on the solid substrate

4.2 Droplet spreading on the solid surface

The spreading phenomenon of the droplet is validated based on the experimental results performed by Bird et al. (2008) [4]. The figure 4(a) shows the spreading behavior of the droplet on the hydrophilic/hydrophobic surface at the same time. In the fig. 4(b), the simulation results are compared with experimental results and the non-dimensional spreading radii according to the non-dimensional time are well predicted.
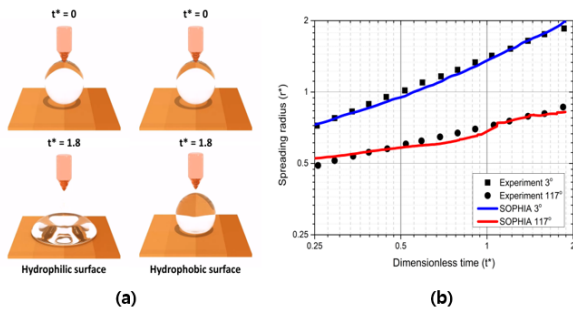

(a)   (b)

Fig. 4. The time evolution of the spreading droplets on hydrophilic/hydrophobic solid surfaces

(a)

4.3 Droplet impact to the dry solid surface at low $We\#$

The droplet motion after the droplet-surface collision is validated. The large variation on the droplet behavior can be shown greatly depending on the wettability of the surface when single droplet collides with a solid surface with a constant velocity. It may rebound or not rebound, and in some cases, it may break and generate some fragments if it collides with a high Weber number. In this section, the spreading behaviors of droplets colliding to the surface with a low Weber number are validated. The figure 5(a) depicts the movements of the droplets after the impact and the contact radii according to the time agree well with the experimental results as in fig. 5(b)..
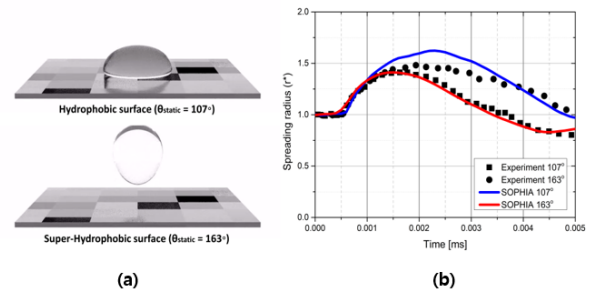

(a)   (b)

Fig. 5. Droplet impact on hydrophobic surface at the low $We^{\#}$

4.3 Droplet impact to the wet solid surface at high $We\#$

Finally, the droplets colliding with a wet surface are simulated without air phase. A thin liquid film (lamella) is generated above the water surface and spreads after the droplet splash on the wet surface. The shape of the water surface at same time instant is shown in fig. 6 (a). The progression of the lamella shows good agreement with the analytical prediction as in fig. 6(b).
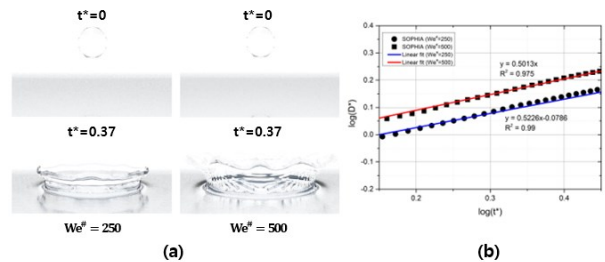

(a)   (b)

Fig. 6. Droplet impact on wet superhydrophobic surface at different $We^{\#}$

5. Summary

In this study, various droplet-surface collision phenomena are analyzed using the 3D SPH model. PFSPH theory is adopted for physical modeling on surface tension and wetting characteristics. The accuracy of the numerical models is verified by the verification of the pressure distribution of a single droplet and different contact angles with different wetting conditions. The numerical model is validated through the numerical studies on droplet-surface spreading and collision phenomena. In addition, the droplet impact on wet surface is carried out and all results show good agreements on experimental results and analytical prediction. It is shown that our numerical model can deal with various droplet-surface impact phenomena that can occur in nuclear engineering fields.

REFERENCES

[1] ZHANG, Huang, et al. Droplet impaction in nuclear installations and safety analysis: Phenomena, findings and approaches. Nuclear Engineering and Design, 2020, 366: 110757.
[2] MONAGHAN, Joe J. Simulating free surface flows with SPH. Journal of computational physics, 1994, 110.2: 399-406.
[3] TARTAKOVSKY, Alexandre M.; PANCHENKO, Alexander. Pairwise force smoothed particle hydrodynamics model for multiphase flow: surface tension and contact line dynamics. Journal of Computational Physics, 2016, 305: 1119-1146.
[4] BIRD, James C.; MANDRE, Shreyas; STONE, Howard A. Short-time dynamics of partial wetting. Physical review letters, 2008, 100.23: 234501.
[5] KIM, Hyungmo, et al. Drop impact characteristics and structure effects of hydrophobic surfaces with micro-and/or nanoscaled structures. Langmuir, 2012, 28.30: 11250-11257.
[6] WEISS, Daniel A.; YARIN, Alexander L. Single drop impact onto liquid films: neck distortion, jetting, tiny bubble entrainment, and crown formation. Journal of Fluid Mechanics, 1999, 385: 229-254.